

# ENSO signature in botanical proxy time series extends terrestrial El Niño record into the (sub)tropics

Timme H. Donders,<sup>1</sup> Surangi W. Punyasena,<sup>2</sup> Hugo J. de Boer,<sup>3</sup>  
and Friederike Wagner-Cremer<sup>1</sup>

Received 16 September 2013; revised 14 October 2013; accepted 16 October 2013; published 12 November 2013.

[1] The El Niño–Southern Oscillation (ENSO) exerts significant control over the amount of Florida winter precipitation. We use a local near-annual resolved palaeobotanical proxy record from southern Florida to test for historic ENSO variability over the past 125 years. Palaeobotanical proxies from a Florida wetland, pollen counts, and a new drought-stress proxy based on leaf epidermal cell densities are used as indicators of moisture availability during the winter growing season. Spectral analysis and band-pass filtering of the proxy records reveal significant variability within the 2–7 year bandwidth characteristic of ENSO, as well as decadal signatures. A maximum likelihood palaeoprecipitation reconstruction of the pollen record based on modern vegetation distributions shows values and variability comparable to instrumental records. The approach shows the dominant control of ENSO on Florida vegetation and provides a powerful means to detect discrete ENSO variability in older intervals.

**Citation:** Donders, T. H., S. W. Punyasena, H. J. de Boer, and F. Wagner-Cremer (2013), ENSO signature in botanical proxy time series extends terrestrial El Niño record into the (sub)tropics, *Geophys. Res. Lett.*, 40, 5776–5781, doi:10.1002/2013GL058038.

## 1. Introduction

[2] Land-based palaeoclimate records are crucial for understanding the impact of past climate change in the terrestrial realm. A particular field of interest is the El Niño–Southern Oscillation (ENSO), which has a global impact on terrestrial systems [Ropelewski and Halpert, 1987; Van Oldenborgh and Burgers, 2005]. Detailed understanding of past ENSO dynamics is crucial for production of better forecasting scenarios and to reconcile palaeoclimate data with model output. The ENSO variability is most prominent on interannual time scales [Allan, 2000; McPhaden, 2003], and thus, climatic proxy data should be ideally analyzed with near-annual resolution to detect the 2–7 year ENSO frequency band. The main impact of ENSO within

terrestrial systems concerns precipitation deficits and surpluses across all continents [Ropelewski and Halpert, 1987]. Regions with the most prominent ENSO impact are located within the Indo-Pacific Warm Pool [Dai and Wigley, 2000], while most major teleconnections are confined to low-latitude (sub)tropical areas, such as the southern U.S. [Vega et al., 1998; Larkin and Harrison, 2005].

[3] Annually resolved ENSO proxies include width and density measurements from tree rings, layer thickness from laminated sediments, and accumulation/isotopic indicators from ice, speleothem, and coral records [Gergis et al., 2006]. High-resolution records, however, are difficult to obtain and often have restricted geographic availability [Markgraf and Diaz, 2000]. Constraints may include a lack of tree species with annual growth rings in low-latitude to midlatitude areas and the restriction of coral records to tropical warm-water regions [Gergis et al., 2006]. To help resolve the scarcity of Holocene annually resolved records [Donders et al., 2008], we test the sensitivity of high-resolution pollen and leaf macrofossil records to ENSO-forced precipitation changes. Because pollen-based reconstructions can be converted in quantitative estimates using surface sample calibration data and, subsequently, compared to model experiment output [see, e.g., Donders et al., 2011], a quantitative measure of the degree of ENSO-forced climate change can be potentially obtained.

### 1.1. High-Resolution Botanical Analysis of Florida Peat Records

[4] We investigate the imprint of ENSO variability in botanical proxies and the stability of the Florida ENSO teleconnection using a 125 year, high-resolution palaeoclimate record from wetland peat deposits in Florida (Figure 1a). Peat deposits are widespread source of fossil plant remains, and their composition is sensitive to hydrological changes [Barber and Charman, 2003]. Plant growth during spring in southern Florida wetlands is strongly influenced by the amount of winter precipitation as the amount of dry season (winter) precipitation determines the hydroperiod length [Donders et al., 2005a, 2005b], which, in turn, is strongly teleconnected to the ENSO cycle [Vega et al., 1998; Larkin and Harrison, 2005].

[5] Precipitation deficits imprint detectable signatures in developing leaves [Wagner-Cremer et al., 2010]. We employ a new proxy for moisture availability during the growing season, i.e., leaf epidermal cell density (ED), in combination with an annually resolved pollen record to reconstruct ENSO-induced water availability. Small dating uncertainties impede direct correlation between the proxy data and ENSO indices [Donders et al., 2004]. However, spectral analysis of independently dated proxy time series provides a means for

Additional supporting information may be found in the online version of this article.

<sup>1</sup>Palaeoecology, Department of Physical Geography, Faculty of Geosciences, Utrecht University, Utrecht, Netherlands.

<sup>2</sup>Department of Plant Biology, University of Illinois at Urbana-Champaign, Urbana, Illinois, USA.

<sup>3</sup>Department of Environmental Sciences, Copernicus Institute, Faculty of Geosciences, Utrecht University, Utrecht, Netherlands.

Corresponding author: T. H. Donders, Palaeoecology, Department of Physical Geography, Utrecht University, Budapestlaan 4, NL-3584 CD Utrecht, Netherlands. (t.h.donders@uu.nl)

©2013. American Geophysical Union. All Rights Reserved.  
0094-8276/13/10.1002/2013GL058038

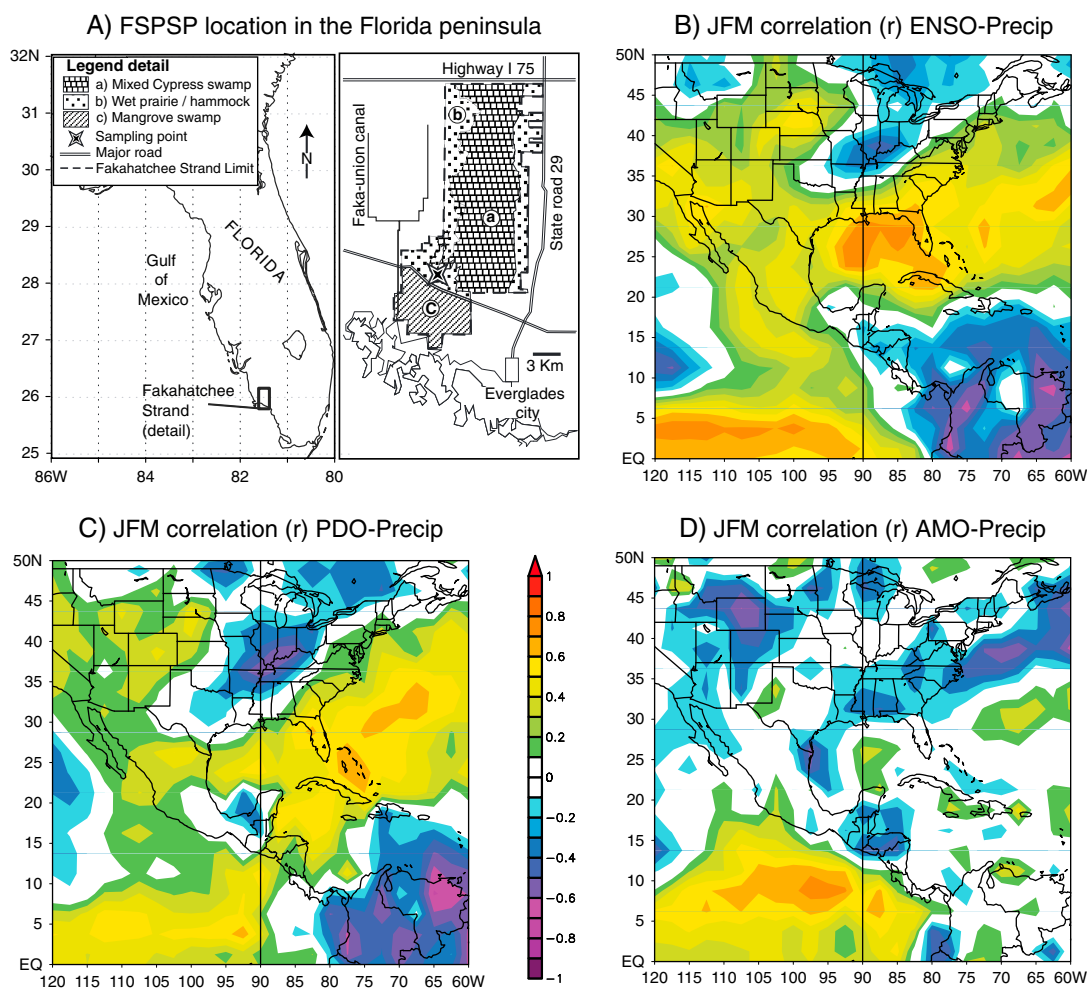


**Figure 1.** (a–d) Influence of global climate oscillations on winter precipitation in the Florida region. Correlation ( $r$ ) between CMAP precipitation data [Xie and Arkin, 1996] and indices for NINO3.4 in Figure 1b, the PDO in Figure 1c, and the AMO in Figure 1d. Figure 1a shows the position and regional setting of coring location in the Fakahatchee Strand wetland in Florida (U.S.).

detecting the distinct signature of ENSO [Rodbell et al., 1999; Moy et al., 2002].

[6] Analysis of herbarium material collected over the past ~100 years has shown that ED on *Quercus laurifolia* leaves increases linearly with decreasing winter precipitation in southern Florida, which is indicative of drought stress sensitivity. Subsequent analysis of subfossil *Q. laurifolia* leaf remains on near-annual resolution provided independent confirmation of this relation, and is independent of CO<sub>2</sub> [Wagner-Cremer et al., 2010]. High-resolution pollen analysis from the same site has shown a clear response to both decadal and near-annual variations in water availability [Donders et al., 2005a].

[7] Furthermore, pollen-trap experiments in widespread regions have revealed dependence of annual pollen deposition on climate variables which, depending on the area, is primarily controlled by temperature and precipitation variability [Green et al., 1988; Hicks, 2001; Willard et al., 2003; Haselhorst et al., 2013]. Here we use this concept to quantify the past 125 years of Florida winter (dry season) precipitation and calibrate observed changes based on a probabilistic model of modern plant taxon distributions

[Punyasena et al., 2008; Punyasena, 2008; Whitney et al., 2011]. Additionally, the variability in the botanical record is compared to regional precipitation patterns associated with the ENSO, the Pacific Decadal Oscillation (PDO), and the Atlantic Multidecadal Oscillation (AMO).

## 2. Proxy Data and Reconstruction Methods

[8] We performed leaf cuticle and pollen analysis on a peat section from the Fakahatchee Strand Preserve State Park (FSPSP), southwest Florida (Figure 1a; see also Text S1 in the supporting information). A series of 10 accelerator mass spectrometry <sup>14</sup>C data were obtained from the 84 cm profile. An accurate chronology was acquired for the last 125 years by performing a combined wiggle-match and <sup>14</sup>C bomb-pulse calibration, with an estimated maximum error of ~5 years [Donders et al., 2004]. The high accumulation rate, i.e., ~0.5 cm yr<sup>-1</sup>, and stable depositional setting provided excellent conditions for performing a palaeoclimatic proxy study on annual resolution. Pollen were analyzed at 0.5 cm intervals (~1 sample yr<sup>-1</sup>) (Figure S1). Results are displayed as the first principal component from the assemblages, which

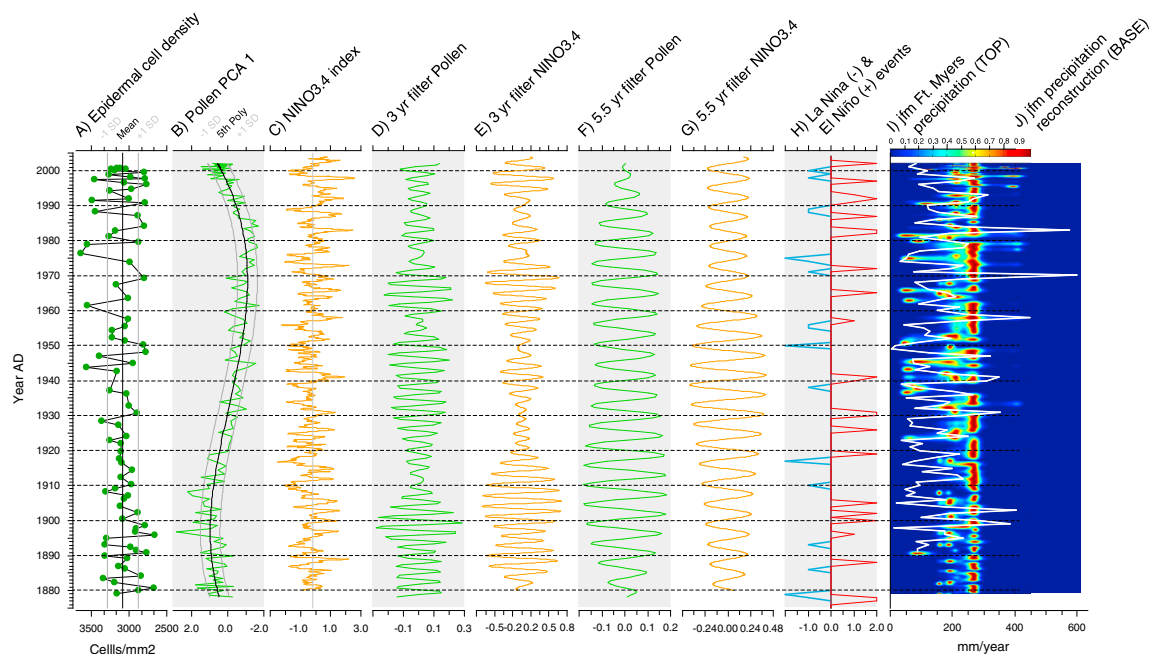


**Figure 2.** Botanical proxy data from the FSPSP peat core compared to NINO3.4 and precipitation forcing. (a) Epidermal cell density (ED) counts from subfossil *Quercus laurifolia* leaf remains, expressed as  $n$  cells  $\text{mm}^{-2}$  (15). (b) First principal component analysis (PCA) axis derived from pollen assemblage data (77.5% of total variance explained; see supporting information). Standard deviation range envelope was calculated on detrended data by fitting a fifth-order polynomial. Positive anomalies of both curves (note reversed axes in Figures 2a and 2b) indicate drier conditions during growing season [Donders et al., 2005a; Wagner-Cremer et al., 2010]. (c) The 5 month running average of the NINO3.4 index [Kaplan et al., 1998]. Band-pass filtered NINO3.4 and pollen data at (d, e) 3 years and (g, h) 5.5 years. (h) ENSO events defined by both the NINO3.4 index and the SOI exceeding the lower (SOI: upper) tercile ( $\pm 1$ ) or, during a strong event, exceeding the twentieth percentile ( $\pm 2$ ) for more than four consecutive months [Smith and Sardeshmukh, 2000]. Independent Y axis for Figures 2a and 2b is based on an age-depth model with 3–5 years accuracy [Donders et al., 2004]. (i) Local JFM precipitation record of nearby Fort Myers, Florida. (j) Reconstructed normalized maximum likelihood JFM precipitation values from pollen data.

represents a ratio between dry and wet taxa at this locality (Figures 2b and S2) and responds to changes in dry season (winter) precipitation [Donders et al., 2005a].

[9] For the quantitative dry (winter) season precipitation reconstruction, modern plant distribution data available through the Global Biodiversity Database (www.gbif.org) were matched with a high-resolution (1 km grid) world climate database for land areas [Hijmans et al., 2005]. Point values of cold quarter precipitation at recorded occurrences were extracted for each taxon. The analysis was performed for 25 key taxa at the same taxonomic resolution to which the pollen taxa were identified (Table S1 and Text S1). Resulting distribution data were individually modeled as kernel probability densities following Punyasena [2008] and Whitney et al. [2011], reflecting the likelihood of finding a given taxon at a specific precipitation value. Likelihood precipitation values of the fossil pollen data then are the summed log likelihoods of the individual taxon distributions in the sample. This approach combines information from both low (family) and high (species) resolution taxonomic units that contribute to the estimate while largely avoiding nonanalogue problems of other compositional-based approaches [Punyasena, 2008].

[10] Regional precipitation patterns were analyzed using merged analyses of global precipitation data [CPC Merged Analysis of Precipitation (CMAP)] [Xie and Arkin, 1996]

using the NOAA Earth System Research Laboratory tool at <http://www.esrl.noaa.gov/psd>. As the local botanical record is most sensitive to winter precipitation [Donders et al., 2005a], we correlated climate indices for the ENSO, the PDO, and the AMO with CMAP winter [January–February–March (JFM)] precipitation averaged from 1979 to 2010. The correlation ( $r$ ) values were plotted for the larger Florida region to illustrate the regional influence of these climate modes (Figures 1b–1d).

### 3. High-Resolution ENSO Record

[11] Winter precipitation in the larger Florida region is positively correlated with the multiannual variability of NINO3.4 (Figure 1b) and the decadal variability of the PDO (Figure 1c). La Niña periods produce drought conditions in southern Florida, while El Niño conditions lead to higher winter precipitation. No direct correlation was found between Florida winter precipitation and the AMO (Figure 1d), although the AMO does modulate the influence of the ENSO on Florida winter precipitation [Enfield et al., 2001].

[12] ED analysis on 82 core samples shows 13 ED peaks above the  $1\sigma$  range between 1879 and 2001 (Figure 2a). Because ED resolution is limited by the availability of leaf material, this would be equivalent to  $\sim 19$  peaks at annual

**Table 1.** Significant Periodicities in the Proxy and Climatic Time Series Reported by Their Main Periodicity and Significance Level Tested With RED FIT [Schulz and Mudelsee, 2002]<sup>a</sup>

Period (years)	Proxy Records			Climate Indices						Precipitation South Florida (Ft. Myers)				
	PCA 1 Pollen		Epidermal Density		NINO3.4		PDO		Annual		DJF		JJA	
	Sign (%)	Period (years)	Sign (%)	Period (years)	Period (years)	Sign (%)	Period (years)	Sign (%)	Period (years)	Sign (%)	Period (years)	Sign (%)	Period (years)	Sign (%)
46	80	17.58	99	56	99	11.8	95	20	80	34	90			
<b>5.7</b>	<b>80</b>	8.39	95	<b>5.7</b>	<b>99</b>	9.5	95	<b>5.6</b>	<b>95</b>	7.8	95			
4.2	90	<b>5.5</b>	<b>90</b>	5.1	80	<b>5.8</b>	<b>90</b>	4.7	95	<b>6.3</b>	<b>80</b>			
<b>2.9</b>	<b>95</b>	4.9	99	4.4	80	<b>3.6</b>	<b>95</b>	<b>3.5</b>	<b>90</b>	5	95			
2.6	95	<b>3.5</b>	<b>99</b>	<b>3.3</b>	<b>95</b>	<b>3.6</b>	<b>95</b>	<b>2.5</b>	<b>90</b>	<b>3.3</b>	<b>95</b>			
1.7	95	<b>3</b>	<b>99</b>	<b>2.9</b>	<b>80</b>	2.1	99	2.3	80	2.1	99			
						2	95			2	95			
						1.74								

<sup>a</sup>Periodicities in bold occur consistently between proxy and climate records.

PCA = Principal component analysis, DJF = December-January-February, JJA = June-July-August.

resolution for the entire profile (Table S2). Between 1879 and 2001, 16 La Niña years have actually occurred, defined by both the NINO3.4 index (Figure 2c) and the Southern Oscillation Index (SOI) exceeding the lower and upper tercile values, respectively, for more than four consecutive months (Figure 2h) [Smith and Sardeshmukh, 2000]. In general, both the leaf cuticle and pollen proxies overestimate La Niña occurrence, while El Niño phases remain slightly underrepresented (Table S2). Most likely, La Niña-induced dry periods have a greater impact on the wetland vegetation of Florida.

### 3.1. Periodicity in Proxy Signal

[13] The ENSO forcing present in the proxy time series was further assessed by RED FIT spectral analysis and bootstrapped significance testing [Schulz and Mudelsee, 2002], which is well suited for unevenly spaced data series (Table 1 and Figure S3). NINO3.4 time series power spectra and local winter precipitation show the prominent ENSO variability between 2 and 7 years, with a triplet of sharp peaks between 2 and 4.5 years and a wide peak around ~5.5 years (Table 1 and Figure S3). Spectral analysis of the proxy data reveals highly similar variability within the ENSO band. In particular, the pollen data contain the prominent high-frequency 2 to 3 ENSO pattern, although the periods do not exactly match the NINO3.4 spectrum. The ED series has a lower sample resolution, and it therefore does not contain the 2–3 year signal, but the remaining periods match the ENSO signature very well and are significant at the 99% confidence limit (Table 1). Band-pass filtering of the most significant spectral peaks in the NINO3.4 and pollen data shows a continuous signal of ~5.5 years throughout the entire record (Figures 2f and 2g). Amplitude variations are highly comparable and suggest that the pollen record captures the dynamics of the ENSO forcing. The ~3 year cycle is not continuously present with the NINO3.4 signal, and this feature is reflected well in the filtered pollen data (Figures 2d and 2e).

[14] Unlike the ED data, the periods from the pollen spectra slightly deviate from the NINO3.4 signal. The lagged response of pollen productivity to climate variations [Willard et al., 2003] might cause these offsets. Alternatively, offsets can be explained by the dating uncertainties, but the effect is likely limited as the main ED and NINO3.4 periods match very closely and cross correlation revealed no phase lag.

[15] Periodicity >7 years seems stronger in the proxy data than in the NINO3.4 and has periods that deviate significantly (Table 1). Consequently, the associated variability is most likely not directly related to ENSO forcing. Decadal-scale variability is present in the local precipitation series (Figure S3). Other regionally significant climatic modes, such as the PDO (Figure 1c), show longer-scale variability (Table 1). Possibly, interference of PDO- and ENSO-scale variability produce the observed signals in the precipitation and proxy time series, but this is not yet conclusive. Alternatively, species-dependent growth dynamics might cause these patterns.

### 3.2. Maximum Likelihood Precipitation Reconstruction

[16] The absolute JFM precipitation reconstruction (Figure 2j) shows comparable values as in the instrumental data (Figure 2i) and captures the main transitions surprisingly well. The upper range of the precipitation variability is somewhat overrepresented, and extreme values are not represented;

hence, some degree of smoothing is inherent in the method. Overall, the dynamics of the reconstructed JFM rainfall agrees well with the instrumental record. Best reconstruction results were obtained by using normalized abundance data of dominant local taxa, excluding aquatics and dominant *Taxodium* (see Text S1). The lower precipitation variability observed in the early twentieth century is captured well in all proxies and quantitative reconstruction.

[17] Our results demonstrate the ability of terrestrial botanical proxies to respond to high-frequency climate variability. The proxy data record the ENSO signature in remarkable detail, as shown by the spectral analysis, even though a sediment sample is not a discrete layer containing a single-year sample. The ENSO system seems to exert strong control on the Florida wetland vegetation, even though mainly the winter precipitation is affected [Vega et al., 1998; Larkin and Harrison, 2005]. Because winter precipitation in Florida is reduced relative to the abundant summer rain, ENSO modulation of the amount of winter precipitation is likely to be an important ecological factor for plant growth. The amount of winter precipitation extends or reduces the annual hydroperiod (inundation length), which is a highly important parameter for plant growth in the local wetlands [Donders et al., 2005a]. The ED is apparently highly sensitive to water deficiencies and surpluses, but data resolution is limited by availability of subfossil leaf material. The pollen responses are not high in amplitude but still capture the typical frequencies of ENSO forcing and can be analyzed at annual resolution. The likelihood reconstructions capture the instrumental winter precipitation variations well, but careful selection of taxa is critical. Based on our analysis, the ENSO teleconnection is apparently a stable feature of the Florida climate during the past 125 years, even though some decadal signal is present, possibly modulating the ENSO teleconnection strength [Cane, 2005].

#### 4. Conclusions and Implications

[18] Based on our near-annual analysis of epidermal cell densities and pollen assemblages in a subfossil peat core, we conclude that ENSO-forced precipitation changes leave a detectable imprint with frequency and amplitude changes characteristic of ENSO. We show for the first time that annual-scale precipitation variability can be reconstructed based on pollen and that the resulting record shows continuous imprint of ENSO forcing on winter precipitation during the past 125 years in Florida, pointing to a stable teleconnection. High-resolution botanical records with sufficient time control allow direct testing of the reduced mid-Holocene ENSO hypothesis [Clement et al., 2000; Donders et al., 2005b] in geographically widespread areas. Furthermore, this method can help to resolve the role of decadal fluctuations in Pacific pressure (PDO) [Deser and Wallace, 1990], which has a similar impact as the ENSO and apparently modulates the ENSO teleconnection strength [Cane, 2005], by extending the instrumental hydrological record in the (sub)tropics.

[19] **Acknowledgments.** The authors are indebted to the Fakahatchee Strand Preserve State Park staff for great cooperation and technical support. Fieldwork support from Ton van Druten, Wolfram Kürschner, and Claire Schreurs was indispensable. This research was supported by the Council of Earth and Life Sciences, Netherlands Organization for Scientific Research (NWO).

[20] The Editor thanks two anonymous reviewers for their assistance in evaluating this paper.

#### References

- Allan, R. J. (2000), ENSO and climatic variability in the past 150 years, in *El Niño and the Southern Oscillation: Multiscale Variability and Global and Regional Impacts*, edited by H. F. Diaz et al., pp. 3–55, Cambridge Univ. Press, Cambridge.
- Barber, K. E., and D. J. Charman (2003), Holocene palaeoclimate records from peatlands, in *Global Change in the Holocene*, edited by A. W. Mackay et al., pp. 210–226, Edward Arnold, London.
- Cane, M. A. (2005), The evolution of El Niño, past and future, *Earth Planet. Sci. Lett.*, *230*, 227–240.
- Clement, A. C., R. Seager, and M. A. Cane (2000), Suppression of El Niño during the mid-Holocene by changes in the Earth's orbit, *Paleoceanography*, *15*(6), 731–737.
- Dai, A., and T. M. L. Wigley (2000), Global patterns of ENSO-induced precipitation, *Geophys. Res. Lett.*, *27*, 1283–1286.
- Deser, C., and J. M. Wallace (1990), Large-scale atmospheric circulation features of warm and cold episodes in the tropical Pacific, *J. Clim.*, *3*, 1254–1281.
- Donders, T. H., F. Wagner, K. Van der Borg, A. F. M. de Jong, and H. Visscher (2004), A novel approach for developing high-resolution sub-fossil peat chronologies with <sup>14</sup>C dating, *Radiocarbon*, *46*(1), 455–463.
- Donders, T. H., F. Wagner, and H. Visscher (2005a), Quantification strategies for human-induced and natural hydrological changes in southern Florida wetland vegetation, *Quat. Res.*, *64*, 333–342.
- Donders, T. H., F. Wagner, D. L. Dilcher, and H. Visscher (2005b), Mid- to late-Holocene El Niño–Southern Oscillation dynamics reflected in the subtropical terrestrial realm, *Proc. Natl. Acad. Sci. U.S.A.*, *102*(31), 10,904–10,908.
- Donders, T. H., F. Wagner-Cremer, and H. Visscher (2008), Integration of proxy data and model scenarios for the mid-Holocene onset of modern ENSO variability, *Quat. Sci. Rev.*, *27*, 571–579.
- Donders, T., H. Boer, W. Finsinger, E. Grimm, S. Dekker, G. Reichert, and F. Wagner-Cremer (2011), Impact of the Atlantic Warm Pool on precipitation and temperature in Florida during North Atlantic cold spells, *Clim. Dyn.*, *36*(1–2), 109–118, doi:10.1007/s00382-009-0702-9.
- Enfield, D. B., A. M. Mestas-Núñez, and P. J. Trimble (2001), The Atlantic Multidecadal Oscillation and its relation to rainfall and river flows in the continental U.S., *Geophys. Res. Lett.*, *28*(10), 2077–2080.
- Gergis, J., K. Braganza, A. Fowler, S. Mooney, and J. Risbey (2006), Reconstructing El Niño/Southern Oscillation (ENSO) from high-resolution palaeoarchives, *J. Quat. Sci.*, *21*(7), 707–722, doi:10.1002/jqs.1070.
- Green, D., G. Singh, H. Polach, D. Moss, J. Banks, and E. A. Geissler (1988), A fine-resolution palaeoecology and palaeoclimatology from South-Eastern Australia, *J. Ecol.*, *76*, 790–806.
- Haselhorst, D. S., J. E. Moreno, and S. W. Punyasena (2013), Variability within the 10-year pollen rain of a seasonal neotropical forest and its implications for paleoenvironmental and phenological research, *PLoS One*, *8*(1), e53485.
- Hicks, S. (2001), The use of annual arboreal pollen deposition values for delimiting tree-lines in the landscape and exploring models of pollen dispersal, *Rev. Palaeobot. Palynol.*, *117*, 1–29.
- Hijmans, R. J., S. E. Cameron, J. L. Parra, P. G. Jones, and A. Jarvis (2005), Very high resolution interpolated climate surfaces for global land areas, *Int. J. Climatol.*, *25*(15), 1965–1978, doi:10.1002/joc.1276.
- Kaplan, A., M. A. Cane, Y. Kushnir, A. C. Clement, M. B. Blumenthal, and B. Rajagopalan (1998), Analyses of global sea surface temperature 1856–1991, *J. Geophys. Res.*, *103*, 18,567–18,589.
- Larkin, N. K., and D. E. Harrison (2005), On the definition of El Niño and associated seasonal average U.S. weather anomalies, *Geophys. Res. Lett.*, *32*(13), L13705, doi:10.1029/2005GL022738.
- Markgraf, V., and H. F. Diaz (2000), The past ENSO record: A synthesis, in *El Niño and the Southern Oscillation: Multiscale Variability and Global and Regional Impacts*, edited by H. F. Diaz et al., pp. 465–488, Cambridge Univ. Press, Cambridge.
- McPhaden, M. J. (2003), Tropical Pacific Ocean heat content variations and ENSO persistence barriers, *Geophys. Res. Lett.*, *30*(9), 1480, doi:10.1029/2003GL016872.
- Moy, C. M., G. O. Seltzer, G. T. Rodbell, and D. M. Anderson (2002), Variability of El Niño/Southern Oscillation activity at millennial time-scales during the Holocene epoch, *Nature*, *420*, 162–165.
- Punyasena, S. W. (2008), Estimating neotropical palaeotemperature and palaeoprecipitation using plant family climatic optima, *Palaeogeogr. Palaeoclimatol. Palaeoecol.*, *265*(3–4), 226–237, doi:10.1016/j.palaeo.2008.04.025.
- Punyasena, S. W., F. E. Mayle, and J. C. McElwain (2008), Quantitative estimates of glacial and Holocene temperature and precipitation change in lowland Amazonian Bolivia, *Geology*, *36*(8), 667–670, doi:10.1130/G24784A.1.

- Rodbell, D. T., G. O. Seltzer, D. M. Anderson, M. B. Abbott, D. B. Enfield, and J. H. Newman (1999), An ~15,000-year record of El Niño-driven alluviation in southwestern Ecuador, *Science*, 283(5401), 516–520.
- Ropelewski, C. F., and M. S. Halpert (1987), Global and regional scale precipitation patterns associated with ENSO, *Mon. Weather Rev.*, 115, 1589–1606.
- Schulz, M., and M. Mudelsee (2002), REDFIT: Estimating red-noise spectra directly from unevenly spaced paleoclimatic time series, *Comput. Geosci.*, 28(3), 421–426, doi:10.1016/S0098-3004(01)00044-9.
- Smith, C. A., and P. Sardeshmukh (2000), The Effect of ENSO on the intraseasonal variance of surface temperature in winter, *Int. J. Climatol.*, 20, 1543–1557.
- Van Oldenborgh, G. J., and G. Burgers (2005), Searching for decadal variations in ENSO precipitation teleconnections, *Geophys. Res. Lett.*, 32(15), L15701, doi:10.1029/2005GL023110.
- Vega, A. J., R. V. Rohli, and K. G. Henderson (1998), The Gulf of Mexico mid-tropospheric response to El Niño an La Niña forcing, *Clim. Res.*, 10, 115–125.
- Wagner-Cremer, F., T. H. Donders, and H. Visscher (2010), Drought stress signals in modern and subfossil *Quercus laurifolia* (Fagaceae) leaves reflect winter precipitation in southern Florida tied to El Niño–Southern Oscillation activity, *Am. J. Bot.*, 97(5), 753–759, doi:10.3732/ajb.0900196.
- Whitney, B. S., F. E. Mayle, S. W. Punyasena, K. A. Fitzpatrick, M. J. Burn, R. Guillen, E. Chavez, D. Mann, R. T. Pennington, and S. E. Metcalfe (2011), A 45 kyr palaeoclimate record from the lowland interior of tropical South America, *Palaeogeogr. Palaeoclimatol. Palaeoecol.*, 307(1–4), 177–192.
- Willard, D. A., T. M. Cronin, and S. Verardo (2003), Late Holocene climate and ecosystem history from Chesapeake Bay sediment cores, *Holocene*, 13, 201–214.
- Xie, P., and P. A. Arkin (1996), Analyses of global monthly precipitation using gauge observations, satellite estimates, and numerical model predictions, *J. Clim.*, 9(4), 840–858, doi:10.1175/1520-0442(1996)009<0840:AOGMPU>2.0.CO;2.